

# 12

## CR Formulation Overview I

## TABLE OF CONTENTS

	Page
§12.1. <b>Introduction</b>	12-3
§12.2. <b>The Emergence of CR</b>	12-3
§12.2.1. Continuum Mechanics Sources . . . . .	12-3
§12.2.2. FEM Sources . . . . .	12-4
§12.2.3. Shadows of the Past . . . . .	12-5
§12.2.4. Linking FEM and CR . . . . .	12-6
§12.2.5. Element Independent CR . . . . .	12-7
§12.3. <b>Corotational Kinematics</b>	12-9
§12.3.1. Configurations . . . . .	12-9
§12.3.2. Coordinate Systems . . . . .	12-9
§12.3.3. Coordinate Transformations . . . . .	12-11
§12.3.4. Rigid Displacements . . . . .	12-11
§12.3.5. Rotator Formulas . . . . .	12-12
§12.3.6. Degrees of Freedom . . . . .	12-12
§12.3.7. EICR Matrices . . . . .	12-13
§12.3.8. Deformational Translations . . . . .	12-16
§12.3.9. Deformational Rotations . . . . .	12-17

**Note:** This and the following Chapters on the CR formulation of geometrically nonlinear FEM are new. References and Appendices for this material have been placed in Appendix R.

### §12.1. Introduction

Three Lagrangian kinematic descriptions are in present use for finite element analysis of geometrically nonlinear structures: (1) Total Lagrangian (TL), (2) Updated Lagrangian (UL), and (3) Corotational (CR). The CR description is the most recent of the three and the least developed one. Unlike the others, its domain of application is limited by *a priori* kinematic assumptions:

$$\boxed{\text{Displacements and rotations may be arbitrarily large, but deformations must be small.}} \quad (12.1)$$

Because of this restriction, CR has not penetrated the major general-purpose FEM codes that cater to nonlinear analysis. A historical sketch of its development is provided in Section 2.

As typical of Lagrangian kinematics, all descriptions: TL, UL and CR, follow the body (or element) as it moves. The *deformed* configuration is any one taken during the analysis process and need not be in equilibrium during a solution process. It is also known as the *current*, *strained* or *spatial* configuration in the literature, and is denoted here by  $\mathcal{C}^D$ . The new ingredient in the CR description is the “splitting” or decomposition of the motion tracking into two components, as illustrated in Figure 12.1.

1. The *base* configuration  $\mathcal{C}^0$  serves as the origin of displacements. If this happens to be one actually taken by the body at the start of the analysis, it is also called *initial* or *undeformed*. The name *material* configuration is used primarily in the continuum mechanics literature.
2. The *corotated* configuration  $\mathcal{C}^R$  varies from element to element (and also from node to node in some CR variants). For each individual element, its CR configuration is obtained through a *rigid body motion* of the element base configuration. The associated coordinate system is Cartesian and follows the element like a “shadow” or “ghost,” prompting names such as *shadow* and *phantom* in the Scandinavian literature. Element deformations are measured with respect to the corotated configuration.

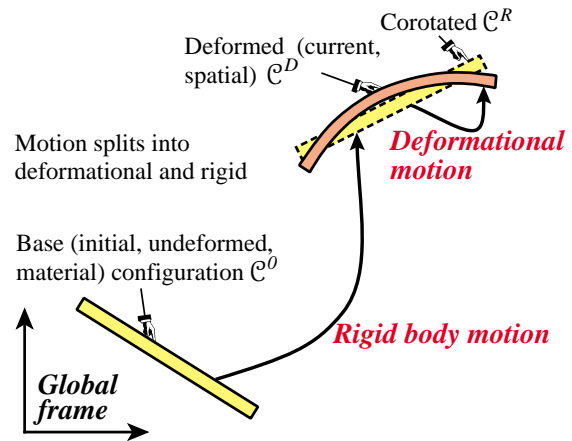


FIGURE 12.1. The CR kinematic description. Deformation from corotated to deformed (current) configuration grossly exaggerated for visibility.

In static problems the base configuration usually remains fixed throughout the analysis. In dynamic analysis the base and corotated configurations are sometimes called the *inertial* and *dynamic* reference configurations, respectively. In this case the base configuration may move at uniform velocity (a Galilean inertial system) following the mean trajectory of an airplane or satellite.

From a mathematical standpoint the explicit presence of a corotated configuration as intermediary between base and current is unnecessary. The motion split may be exhibited in principle as a multiplicative decomposition of the displacement field. The device is nonetheless useful to teach not only the physical meaning but to visualize the strengths and limitations of the CR description.

## §12.2. The Emergence of CR

The CR formulation represents a confluence of developments in continuum mechanics, treatment of finite rotations, nonlinear finite element analysis and body-shadowing methods.

### §12.2.1. Continuum Mechanics Sources

In continuum mechanics the term “corotational” (often spelled “co-rotational”) appears to be first mentioned in Truesdell and Toupin’s influential exposition of field theories [R.81, Sec. 148]. It is used there to identify Jaumann’s stress flux rate, introduced in 1903 by Zaremba. By 1955 this rate had been incorporated in hypoelasticity [R.82] along with other invariant flux measures. Analogous differential forms have been used to model endochronic plasticity [R.85]. Models labeled “co-rotational” have been used in rheology of non-Newtonian fluids; cf. [R.17,R.78]. These continuum models place no major restrictions on strain magnitude. Constraints of that form, however, have been essential to make the idea practical in nonlinear structural FEA, as discussed below.

The problem of handling three-dimensional finite rotations in continuum mechanics is important in all Lagrangian kinematic descriptions. The challenge has spawned numerous publications, for example [R.1,R.4,R.5,R.34,R.42,R.43,R.62,R.71,R.72]. For use of finite rotations in mathematical models, particularly shells, see [R.60,R.70,R.77]. There has been an Euromech Colloquium devoted entirely to that topic [R.61].

The term “corotational” in a FEM paper title was apparently first used by Belytschko and Glaum [R.8]. The survey article by Belytschko [R.9] discusses the concept from the standpoint of continuum mechanics.

### §12.2.2. FEM Sources

In the Introduction of a key contribution, Nour-Omid and Rankin [R.54] attribute the original concept of corotational procedures in FEM to Wempner [R.86] and Belytschko and Hsieh [R.7].

The idea of a CR frame attached to individual elements was introduced by Horrigmoe and Bergan [R.39,R.40]. This activity continued briskly under Bergan at NTH-Trondheim with contributions by Kråkeland [R.46], Nygård [R.15,R.56,R.57], Mathisen [R.48,R.49], Levold [R.47] and Bjærum [R.18]. It was summarized in a 1989 review article [R.56]. Throughout this work the CR configuration is labeled as either “shadow element” or “ghost-reference.” As previously noted the device is not mathematically necessary but provides a convenient visualization tool to explain CR. The shadow element functions as intermediary that separates rigid and deformational motions, the latter being used to determine the element energy and internal force. However the variation of the forces in a rotating frame was not directly used in the formation of the tangent stiffness, leading to a loss of consistency. Crisfield [R.22–R.24] developed the concept of “consistent CR formulation” where the stiffness matrix appears as the true variation of the internal force. An approach blending the TL, UL and CR descriptions was investigated in the mid-1980s at Chalmers [R.50–R.52].

In 1986 Rankin and Brogan at Lockheed introduced [R.63] the concept of “element independent CR formulation” or EICR, which is further discussed below. The formulation relies heavily on the use of projection operators, without any explicit use of “shadow” configurations. It was further refined by Rankin, Nour-Omid and coworkers [R.54,R.64–R.67], and became essential part of the nonlinear shell analysis program STAGS [R.68].

The thesis of Haugen on nonlinear thin shell analysis [R.37] resulted in the development of the formulation discussed in this article. This framework is able to generate a set of hierarchical CR formulations. The work combines tools from the EICR (projectors and spins) with the shadow element concept and assumed

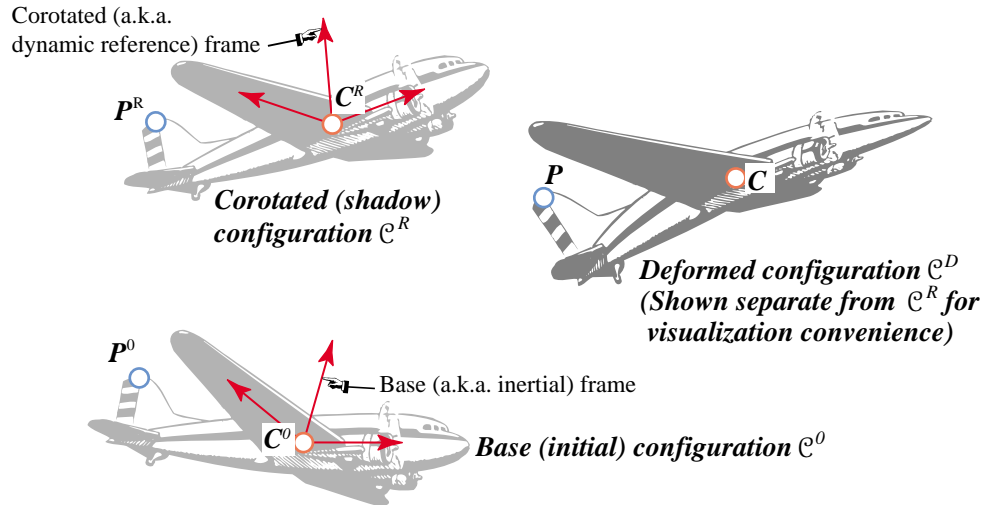


FIGURE 12.2. The concept of separation of base (a.k.a. inertial) and CR (a.k.a. dynamic) configurations in aircraft dynamics. Deformed configuration (with deformations grossly exaggerated) shown separate from CR configuration for visibility. In reality points  $C$  and  $C^R$  coincide.

strain element formulations. Spins (instead of rotations) are used as incremental nodal freedoms. This simplifies the EICR “front end” and facilitates attaining consistency.

Battini and Pacoste at KTH-Stockholm [R.2,R.3,R.58] have recently used the CR approach, focusing on stability applications. The work by Teigen [R.79] should be cited for the careful use of offset nodes linked to element nodes by eccentricity vectors in the CR modeling of prestressed reinforced-concrete members.

### §12.2.3. Shadows of the Past

The CR approach has also roots on an old idea that precedes FEM by over a century: the separation of rigid body and purely deformational motions in continuum mechanics. The topic arose in theories of small strains superposed on large rigid motions. Truesdell [R.80, Sec. 55] traces the subject back to Cauchy in 1827. In the late 1930s Biot advocated the use of incremental deformations on an initially stressed body by using a truncated polar decomposition. However this work, collected in a 1965 monograph [R.16], was largely ignored as it was written in an episodic manner, using full notation by then out of fashion. A rigorous outline of the subject is given in [R.83, Sec. 68] but without application examples.

Technological applications of this idea surged after WWII from a totally different quarter: the aerospace industry. The rigid-plus-deformational decomposition idea for an *entire structure* was originally used by aerospace designers in the 1950s and 1960s in the context of dynamics and control of orbiting spacecraft as well as aircraft structures. The primary motivation was to trace the mean motion.

The approach was systematized by Fraeijns de Veubeke [R.25], in a paper that essentially closed the subject as regards handling of a complete structure. The motivation was clearly stated in the Introduction of that article, which appeared shortly before the author’s untimely death:

“The formulation of the motion of a flexible body as a continuum through inertial space is unsatisfactory from several viewpoints. One is usually not interested in the details of this motion but in its main characteristics such as the motion of the center of mass and, under the assumptions that the deformations remain small, the history of the average orientation of the body. The last information is of course essential to pilots, real and artificial, in order to implement guidance corrections. We therefore try to define a set of Cartesian mean axes accompanying the body, or dynamic reference frame, with respect to which the relative displacements,

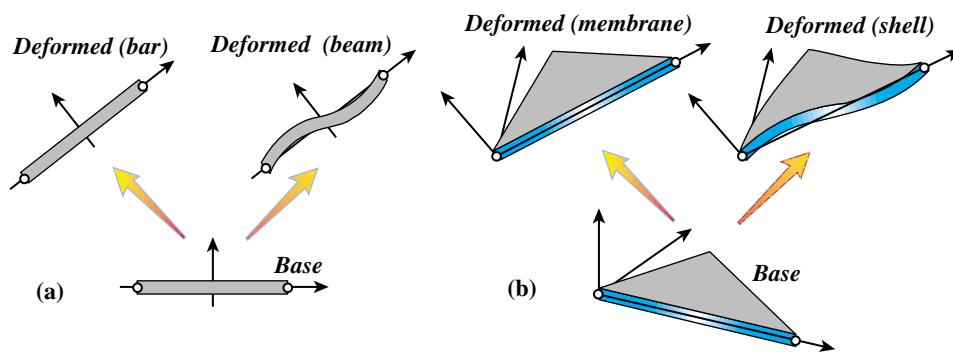


FIGURE 12.3. Geometric tracking of CR frame: (a) Bar or beam element in 2D; (b) Membrane or shell element in 3D.

velocities or accelerations of material points due to the deformations are minimum in some global sense. If the body does not deform, any set of axes fixed into the body is of course a natural dynamic reference frame.”

Clearly the focus of this article was on a whole structure, as illustrated in Figure 12.2 for an airplane. This will be called the *shadowing problem*. A body moves to another position in space: find its mean rigid body motion and use this information to locate and orient a corotated Cartesian frame.

Posing the shadowing problem in three dimensions requires fairly advanced mathematics. Using two “best fit” criteria Fraeijs de Veubeke showed that the origin of the dynamic frame must remain at the center of mass of the displaced structure:  $C^R$  in Figure 12.2. However, the orientation of this frame leads to an eigenvalue problem that may exhibit multiple solutions due to symmetries, leading to non uniqueness. (This is obvious by thinking of the polar and singular-value decompositions, which were not used in that article.) That this is not a rare occurrence is demonstrated by considering rockets, satellites or antennas, which often have axisymmetric shape.

**Remark 12.1.** Only  $C^D$  (shown in darker shade in Figure 12.2) is an *actual* configuration taken by the pictured aircraft structure. Both reference configurations  $C^0$  and  $C^R$  are *virtual* in the sense that they are not generally occupied by the body at any instance. This is in contrast to the FEM version of this idea.

#### §12.2.4. Linking FEM and CR

The practical extension of Fraeijs de Veubeke’s idea to geometrically nonlinear structural analysis by FEM relies on two modifications:

1. *Multiple Frames.* Instead of one CR frame for the whole structure, there is one per element. This is renamed the *CR element frame*.
2. *Geometric-Based RBM Separation.* The rigid body motion is separated directly from the total element motion using elementary geometric methods. For example in a 2-node bar or beam one axis is defined by the displaced nodes, while for a 3-node triangle two axes are defined by the plane passing through the points. See Figure 12.3.

The first modification is essential to success. It helps to fulfill assumption (12.1): the element deformational displacements and rotations remain *small* with respect to the CR frame. If this assumption is violated for a coarse discretization, break it into more elements. Small deformations are the key to *element reuse* in the EICR discussed below. If intrinsically large strains occur, however, the breakdown prescription fails. In that case CR offers no advantages over TL or UL.

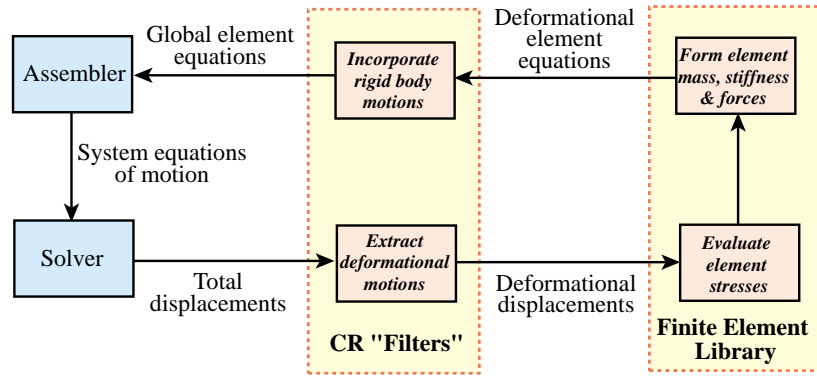


FIGURE 12.4. The EICR as a modular interface to a linear FEM library. The flowchart is mainly conceptual. For computational efficiency the interface logic may be embedded with each element through inlining techniques.

The second modification is inessential. Its purpose is to speed up the implementation of geometrically simple elements. The CR frame determination may be refined later, using more advanced tools such as polar decomposition and best-fit criteria, if warranted.

**Remark 12.2.** CR is occasionally confused with the *convected-coordinate* description of motion, which is used in branches of fluid mechanics and rheology. Both may be subsumed within the class of *moving coordinate* kinematic descriptions. The CR description, however, *maintains orthogonality* of the moving frame(s) thus achieving an exact decomposition of rigid-body and deformational motions. This property enhances computational efficiency as transformation inverses become transposes. On the other hand, convected coordinates form a curvilinear system that “fits” the change of metric as the body deforms. The difference tends to disappear as the discretization becomes progressively finer, but the fact remains that the convected metric must encompass deformations. Such deformations are more important in solid than in fluid mechanics (because classical fluid models “forget” displacements). The idea finds more use in UL descriptions, in which the individual element metric is updated as the motion progresses.

### §12.2.5. Element Independent CR

As previously noted, one of the sources of the present work is the element-independent corotational (EICR) description developed by Rankin and coworkers [R.54,R.63–R.67]. Here is a summary description taken from the Introduction to [R.54]:

“In the co-rotation approach, the deformational part of the displacement is extracted by purging the rigid body components before any element computation is performed. This pre-processing of the displacements may be performed outside the standard element routines and thus is independent of element type (except for slight distinctions between beams, triangular and quadrilateral elements).”

Why is the EICR worth study? The question fits in a wider topic: why CR? That is, what can CR do that TL or UL cannot? The topic is elaborated in the Conclusions section, but we advance a practical reason: *reuse of small-strain elements*, including possibly *materially nonlinear* elements.

The qualifier *element independent* does not imply that the CR equations are independent of the FEM discretization. Rather it emphasizes that the key operations of adding and removing rigid body motions can be visualized as a *front end filter* that lies between the assembler/solver and the element library, as sketched in Figure 12.4. The filter is purely geometric. For example, suppose that a program has four different triangular shell elements with the same node and degree-of-freedom configuration. Then the

**Table 12.1 Configurations in Nonlinear Static Analysis by Incremental-Iterative Methods**

<i>Name</i>	<i>Alias</i>	<i>Explanation</i>	<i>Equilibrium Required?</i>	<i>Identification</i>
Generic	Admissible	A kinematically admissible configuration	No	$\mathcal{C}$
Perturbed		Kinematically admissible variation of a generic configuration.	No	$\mathcal{C} + \delta\mathcal{C}$
Deformed	Current Spatial	Actual configuration taken during the analysis process. Contains others as special cases.	No	$\mathcal{C}^D$
Base*	Initial Undeformed Material	The configuration defined as the origin of displacements.	Yes	$\mathcal{C}^0$
Reference		Configuration to which computations are referred	TL,UL: Yes. CR: $\mathcal{C}^R$ no, $\mathcal{C}^0$ yes	TL: $\mathcal{C}^0$ , UL: $\mathcal{C}^{n-1}$ , CR: $\mathcal{C}^R$ and $\mathcal{C}^0$
Iterated†		Configuration taken at the $k^{th}$ iteration of the $n^{th}$ increment step	No	$\mathcal{C}_k^n$
Target†		Equilibrium configuration accepted at the $n^{th}$ increment step	Yes	$\mathcal{C}^n$
Corotated‡	Shadow Ghost	Body or element-attached configuration obtained from $\mathcal{C}^0$ through a rigid body motion (CR description only)	No	$\mathcal{C}^R$
Globally-aligned	Connector	Corotated configuration forced to align with the global axes. Used as “connector” in explaining the CR description.	No	$\mathcal{C}^G$

\*  $\mathcal{C}^0$  is often the same as the *natural state* in which body (or element) is undeformed and stress-free.  
† Used only in Part II [R.38] in the description of solution procedures.  
‡ In dynamic analysis  $\mathcal{C}^0$  and  $\mathcal{C}^R$  are called the inertial and dynamic-reference configurations, respectively, when they apply to the entire structure.

front end operations are identical for all four. Adding a fifth small-strain element of this type incurs relatively little extra work to “make it geometrically nonlinear.”

This modular organization is of interest because it implies that the element library of an existing FEM program being converted to the CR description need not be drastically modified, *as long as the analysis is confined to small deformations*. Since that library is typically the most voluminous and expensive part of a production FEM code, *element reuse* is a key advantage because it protects a significant investment. For a large-scale commercial code, the investment may be thousands of man-years.

Of course modularity and computational efficiency can be conflicting attributes. Thus in practice the front end logic may be embedded with each element through techniques such as code inlining. If so the flowchart of Figure 12.4 should be interpreted as conceptual.

### §12.3. Corotational Kinematics

This section outlines CR kinematics of finite elements, collecting the most important relations. Mathematical derivations pertaining to finite rotations are consigned to Appendix A. The presentation assumes static analysis, with deviations for dynamics briefly noted where appropriate.

#### §12.3.1. Configurations

To describe Lagrangian kinematics it is convenient to introduce a rich nomenclature for configurations. For the reader's convenience those used in geometrically nonlinear static analysis using the TL, UL or CR descriptions are collected in Table 12.1. Three: base, corotated and deformed, have already been introduced. Two more: iterated and target, are connected to the incremental-iterative solution process covered in Part II [R.38]. The generic configuration is used as placeholder for any kinematically admissible one. The perturbed configuration is used in variational derivations of FEM equations.

Two remain: reference and globally-aligned. The *reference configuration* is that to which element computations are referred. This depends on the description chosen. For Total Lagrangian (TL) the reference is base configuration. For Updated Lagrangian (UL) it is the converged or accepted solution of the previous increment. For corotational (CR) the reference splits into CR and base configurations.

The *globally-aligned configuration* is a special corotated configuration: a rigid motion of the base that makes the body or element align with the global axes introduced below. This is used as a “connector” device to teach the CR description, and does not imply the body ever occupies that configuration.

The separation of rigid and deformational components of motion is done at the element level. As noted previously, techniques for doing this have varied according to the taste and background of the investigators that developed those formulations. The approach covered here uses shadowing and projectors.

#### §12.3.2. Coordinate Systems

A typical finite element, undergoing 2D motion to help visualization, is shown in Figure 12.5. This diagram as well as that of Figure 12.6 introduces kinematic quantities. For the most part the notation follows that used by Haugen [R.37], with subscripting changes.

Configurations taken by the element during the response analysis are linked by a Cartesian *global frame*, to which all computations are ultimately referred. There are actually two such frames: the *material global frame* with axes  $\{X_i\}$  and position vector  $\mathbf{X}$ , and the *spatial global frame* with axes  $\{x_i\}$  and position vector  $\mathbf{x}$ . The material frame tracks the base configuration whereas the spatial frame tracks the CR and deformed (current) configurations. The distinction agrees with the usual conventions of dual-tensor continuum mechanics [R.81, Sec. 13]. Here both frames are taken to be *identical*, since for small strains nothing is gained by separating them (as is the case, for example, in the TL description). Thus only one set of global axes, with dual labels, is drawn in Figures 12.5 and 12.6.

Lower case coordinate symbols such as  $\mathbf{x}$  are used throughout most of the paper. Occasionally it is convenient for clarity to use upper case coordinates for the base configuration, as in Appendix C.

The global frame is the same for all elements. By contrast, each element  $e$  is assigned two local Cartesian frames, one fixed and one moving:

$\{\tilde{x}_i\}$  The element *base frame* (blue in Figure 12.5). It is oriented by three unit base vectors  $\mathbf{i}_i^0$ , which are rows of a  $3 \times 3$  orthogonal rotation matrix (rotator)  $\mathbf{T}_0$ , or equivalently columns of  $\mathbf{T}_0^T$ .

$\{\bar{x}_i\}$  The element *corotated or CR frame* (red in Figure 12.5). It is oriented by three unit base vectors  $\mathbf{i}_i^R$ , which are rows of a  $3 \times 3$  orthogonal rotation matrix (rotator)  $\mathbf{T}_R$ , or equivalently columns of  $\mathbf{T}_0^T$ .

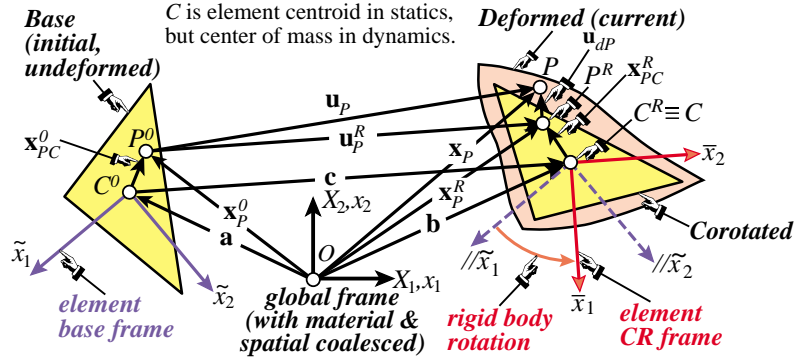


FIGURE 12.5. CR element kinematics, focusing on the motion of generic point  $P$ . Two-dimensional kinematics pictured for visualization convenience.

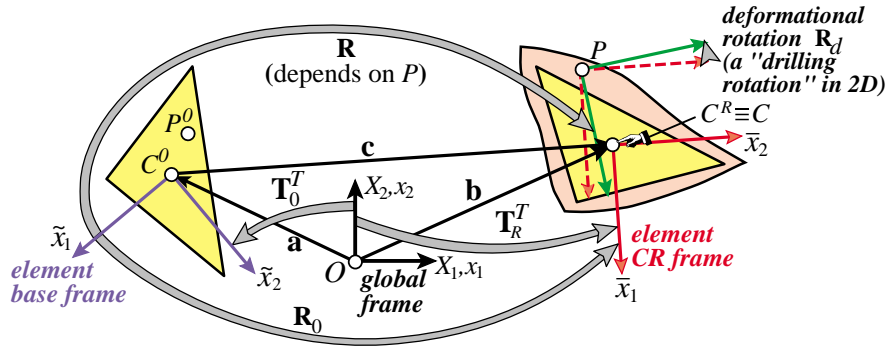


FIGURE 12.6. CR element kinematics, focusing on rotational transformation between frames.

Note that the element index  $e$  has been suppressed to reduced clutter. That convention will be followed throughout unless identification with elements is important. In that case  $e$  is placed as superscript.

The base frame  $\{\tilde{x}_i\}$  is chosen according to usual FEM practices. For example, in a 2-node spatial beam element,  $\tilde{x}_1$  is defined by the two end nodes whereas  $\tilde{x}_2$  and  $\tilde{x}_3$  lie along principal inertia directions. An important convention, however, is that the origin is always placed at the element centroid  $C^0$ . For each deformed (current) element configuration, a fitting of the base element defines its CR configuration, also known as the element “shadow.” Centroids  $C^R$  and  $C \equiv C^D$  coincide. The CR frame  $\{\bar{x}_i\}$  originates at  $C^R$ . Its orientation results from matching a rigid motion of the base frame, as discussed later. When the current element configuration reduces to the base at the start of the analysis, the base and CR frames coalesce:  $\{\tilde{x}_i \equiv \bar{x}_i\}$ . At that moment there are only two different frames: global and local, which agrees with linear FEM analysis.

Notational conventions: use of  $G$ ,  $0$ ,  $R$  and  $D$  as superscripts or subscripts indicate pertinence to the globally-aligned, base, corotated and deformed configurations, respectively. Symbols with a overtilde or overbar are measured to the base frame  $\{\tilde{x}_i\}$  or the CR frame  $\{\bar{x}_i\}$ , respectively. Vectors without a superposed symbol are referred to global coordinates  $\{x_i \equiv x_i\}$ . Examples:  $\mathbf{x}^R$  denote global coordinates of a point in  $\mathcal{C}^R$  whereas  $\tilde{\mathbf{x}}^G$  denote base coordinates of a point in  $\mathcal{C}^G$ . Symbols  $\mathbf{a}$ ,  $\mathbf{b}$  and  $\mathbf{c} = \mathbf{b} - \mathbf{a}$  are abbreviations for the centroidal translations depicted in Figure 12.5, and more clearly in Figure 12.7(b). A generic, coordinate-free vector is denoted by a superposed arrow, for example  $\bar{\mathbf{u}}$ , but such entities rarely appear in this work.

The rotators  $\mathbf{T}_0$  and  $\mathbf{T}_R$  are the well known local-to-global displacement transformations of FEM analysis.

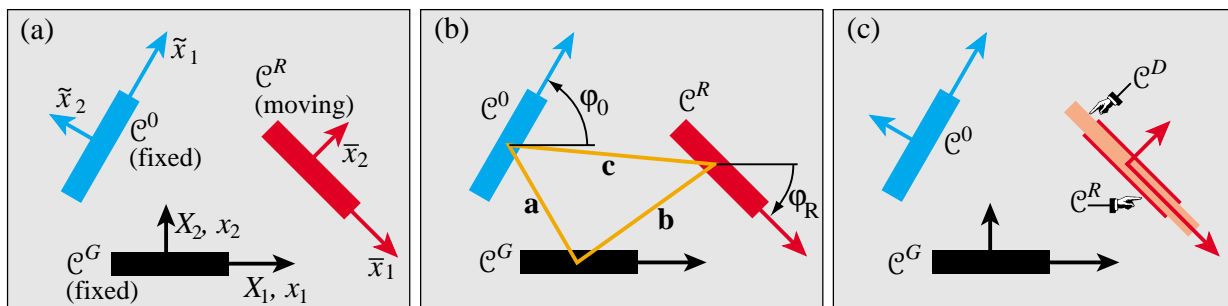


FIGURE 12.7. Further distillation to essentials of Figure 12.5. A bar moving in 2D is shown: (a) Rigid motion from globally-aligned to base and corotated configurations; (b) key geometric quantities that define rigid motions in 2D; (c) as in (a) but followed by a stretch from corotated to deformed. The globally-aligned configuration is fictitious: only a convenient link up device.

Given a global displacement  $\mathbf{u}$ ,  $\tilde{\mathbf{u}} = \mathbf{T}_0 \mathbf{u}$  and  $\bar{\mathbf{u}} = \mathbf{T}_R \mathbf{u}$ .

### §12.3.3. Coordinate Transformations

Figures 12.5 and 12.6, although purportedly restricted to 2D, are still too busy. Figure 12.7, which pictures the 2D motion of a bar in 3 frames, displays essentials better. The (fictitious) globally-aligned configuration  $\mathcal{C}^G$  is explicitly shown. This helps to follow the ensuing sequence of geometric relations.

Begin with a generic point  $\mathbf{x}^G$  in  $\mathcal{C}^G$ . This point is mapped to global coordinates  $\mathbf{x}^0$  and  $\mathbf{x}^R$  in the base and corotated configurations  $\mathcal{C}^0$  and  $\mathcal{C}^R$ , respectively, through

$$\mathbf{x}^0 = \mathbf{T}_0^T \mathbf{x}^G + \mathbf{a}, \quad \mathbf{x}^R = \mathbf{T}_R^T \mathbf{x}^G + \mathbf{b}, \quad (12.2)$$

in which rotators  $\mathbf{T}_0$  and  $\mathbf{T}_R$  were introduced in the previous subsection. To facilitate code checking, for the 2D motion pictured in Figure 12.7(b) the global rotators are

$$\mathbf{T}_0 = \begin{bmatrix} c_0 & s_0 & 0 \\ -s_0 & c_0 & 0 \\ 0 & 0 & 1 \end{bmatrix}, \quad \mathbf{T}_R = \begin{bmatrix} c_R & s_R & 0 \\ -s_R & c_R & 0 \\ 0 & 0 & 1 \end{bmatrix}, \quad c_0 = \cos \varphi_0, \quad s_0 = \sin \varphi_0, \text{ etc.} \quad (12.3)$$

When (12.2) are transformed to the base and corotated frames, the position vector  $\mathbf{x}^G$  must repeat:  $\tilde{\mathbf{x}}^0 = \mathbf{x}^G$  and  $\bar{\mathbf{x}}^R = \mathbf{x}^G$ , because the motion pictured in Figure 12.7(a) is rigid. This condition requires

$$\tilde{\mathbf{x}}^0 = \mathbf{T}_0 (\mathbf{x}^0 - \mathbf{a}), \quad \bar{\mathbf{x}}^R = \mathbf{T}_R (\mathbf{x}^R - \mathbf{b}). \quad (12.4)$$

These may be checked by inserting  $\mathbf{x}^0$  and  $\mathbf{x}^R$  from (12.2) and noting that  $\mathbf{x}^G$  repeats.

### §12.3.4. Rigid Displacements

The rigid displacement is a vector joining corresponding points in  $\mathcal{C}^0$  and  $\mathcal{C}^R$ . This may be referred to the global, base or corotated frames. For convenience call the  $\mathcal{C}^0 \rightarrow \mathcal{C}^R$  rotator  $\mathbf{R}_0 = \mathbf{T}_R^T \mathbf{T}_0$ . Also introduce  $\tilde{\mathbf{c}} = \mathbf{T}_0^T \mathbf{c}$  and  $\bar{\mathbf{c}} = \mathbf{T}_R^T \mathbf{c}$ . Some useful expressions are

$$\begin{aligned} \mathbf{u}_r &= \mathbf{x}^R - \mathbf{x}^0 = (\mathbf{T}_R^T - \mathbf{T}_0^T) \mathbf{x}^G + \mathbf{c} = (\mathbf{R}_0 - \mathbf{I}) \mathbf{T}_0^T \mathbf{x}^G + \mathbf{c} = (\mathbf{R}_0 - \mathbf{I}) \mathbf{T}_0^T \tilde{\mathbf{x}}^0 + \mathbf{c} \\ &= (\mathbf{R}_0 - \mathbf{I}) \mathbf{T}_0^T \bar{\mathbf{x}}^R + \mathbf{c} = (\mathbf{R}_0 - \mathbf{I}) (\mathbf{x}^0 - \mathbf{a}) + \mathbf{c} = (\mathbf{I} - \mathbf{R}_0^T) (\mathbf{x}^R - \mathbf{b}) + \mathbf{c}, \\ \tilde{\mathbf{u}}_r &= \mathbf{T}_0 \mathbf{u}_r = \mathbf{T}_0 (\mathbf{R}_0 - \mathbf{I}) \mathbf{T}_0^T \tilde{\mathbf{x}}^0 + \tilde{\mathbf{c}} = (\tilde{\mathbf{R}}_0 - \mathbf{I}) \tilde{\mathbf{x}}^0 + \tilde{\mathbf{c}}, \\ \bar{\mathbf{u}}_r &= \mathbf{T}_R \mathbf{u}_r = \mathbf{T}_R (\mathbf{I} - \mathbf{R}_0^T) \mathbf{T}_R^T \bar{\mathbf{x}}^R + \bar{\mathbf{c}} = (\mathbf{I} - \bar{\mathbf{R}}_0^T) \bar{\mathbf{x}}^R + \bar{\mathbf{c}}. \end{aligned} \quad (12.5)$$

Here  $\mathbf{I}$  is the  $3 \times 3$  identity matrix, whereas  $\tilde{\mathbf{R}}_0 = \mathbf{T}_0 \mathbf{R}_0 \mathbf{T}_0^T$  and  $\bar{\mathbf{R}}_0 = \mathbf{T}_R \mathbf{R}_0 \mathbf{T}_R^T$  denote the  $\mathcal{C}^0 \rightarrow \mathcal{C}^R$  rotator referred to the base and corotated frames, respectively.

### §12.3.5. Rotator Formulas

Traversing the links pictured in Figure 12.8 shows that any rotator can be expressed in terms of the other two:

$$\mathbf{T}_0 = \mathbf{T}_R \mathbf{R}_0, \quad \mathbf{T}_R = \mathbf{T}_0 \mathbf{R}_0^T, \quad \mathbf{R}_0 = \mathbf{T}_R^T \mathbf{T}_0, \quad \mathbf{R}_0^T = \mathbf{T}_0^T \mathbf{T}_R. \quad (12.6)$$

In the CR frame:  $\bar{\mathbf{R}}_0 = \mathbf{T}_R \mathbf{R}_0 \mathbf{T}_R^T$ , whence

$$\bar{\mathbf{R}}_0 = \mathbf{T}_0 \mathbf{T}_R^T, \quad \bar{\mathbf{R}}_0^T = \mathbf{T}_R \mathbf{T}_0^T. \quad (12.7)$$

Notice that  $\mathbf{T}_0$  is fixed since  $\mathcal{C}^G$  and  $\mathcal{C}^0$  are fixed throughout the analysis, whereas  $\mathbf{T}_R$  and  $\mathbf{R}_0$  change. Their variations of these rotators are subjected to the following constraints:

$$\begin{aligned} \delta \mathbf{T}_0 &= \delta \mathbf{T}_0^T = \mathbf{0}, & \delta \mathbf{T}_R &= \mathbf{T}_0 \delta \mathbf{R}_0^T, & \delta \mathbf{T}_R^T &= \delta \mathbf{R}_0 \mathbf{T}_0^T, & \delta \mathbf{R}_0 &= \delta \mathbf{T}_R^T \mathbf{T}_0, \\ \delta \mathbf{R}_0^T &= \mathbf{T}_0^T \delta \mathbf{T}_R, & \mathbf{T}_R^T \delta \mathbf{T}_R + \delta \mathbf{T}_R^T \mathbf{T}_R &= \mathbf{0}, & \mathbf{R}_0^T \delta \mathbf{R}_0 + \delta \mathbf{R}_0^T \mathbf{R}_0 &= \mathbf{0}. \end{aligned} \quad (12.8)$$

The last two come from the orthogonality conditions  $\mathbf{T}_R^T \mathbf{T}_R = \mathbf{I}$  and  $\mathbf{R}_0^T \mathbf{R}_0 = \mathbf{I}$ , respectively, and provide  $\delta \mathbf{R}_0 = -\mathbf{R}_0 \delta \mathbf{R}_0^T \mathbf{R}_0$ ,  $\delta \mathbf{R}_0^T = -\mathbf{R}_0^T \delta \mathbf{R}_0 \mathbf{R}_0^T$ , etc.

We denote by  $\boldsymbol{\omega}$  and  $\bar{\boldsymbol{\omega}}$  the axial vectors of  $\mathbf{R}_0$  and  $\bar{\mathbf{R}}_0$ , respectively, using the exponential map form of the rotator described in Section A.10. The variations  $\delta \boldsymbol{\omega}$  and  $\delta \bar{\boldsymbol{\omega}}$  are used to form the skew-symmetric spin matrices  $\mathbf{Spin}(\delta \boldsymbol{\omega}) = \delta \mathbf{R}_0 \mathbf{R}_0^T = -\mathbf{Spin}(\delta \boldsymbol{\omega})^T$  and  $\mathbf{Spin}(\delta \bar{\boldsymbol{\omega}}) = \delta \bar{\mathbf{R}}_0 \bar{\mathbf{R}}_0^T = -\mathbf{Spin}(\delta \bar{\boldsymbol{\omega}})^T$ . These matrices are connected by congruential transformations:

$$\mathbf{Spin}(\delta \boldsymbol{\omega}) = \mathbf{T}_0^T \mathbf{Spin}(\delta \bar{\boldsymbol{\omega}}) \mathbf{T}_0, \quad \mathbf{Spin}(\delta \bar{\boldsymbol{\omega}}) = \mathbf{T}_0 \mathbf{Spin}(\delta \boldsymbol{\omega}) \mathbf{T}_0^T. \quad (12.9)$$

Using these relations the following catalog of rotator variation formulas can be assembled:

$$\begin{aligned} \delta \mathbf{T}_R &= \mathbf{T}_0 \delta \mathbf{R}_0^T = -\mathbf{T}_R \delta \mathbf{R}_0 \mathbf{R}_0^T = -\mathbf{T}_R \mathbf{Spin}(\delta \boldsymbol{\omega}) = -\mathbf{R}_0^T \mathbf{Spin}(\delta \bar{\boldsymbol{\omega}}) \mathbf{T}_0, \\ \delta \mathbf{T}_R^T &= \delta \mathbf{R}_0 \mathbf{T}_0^T = -\mathbf{R}_0 \delta \mathbf{R}_0^T \mathbf{T}_0^T = \mathbf{Spin}(\delta \boldsymbol{\omega}) \mathbf{T}_R^T = \mathbf{T}_0^T \mathbf{Spin}(\delta \bar{\boldsymbol{\omega}}) \mathbf{R}_0, \\ \delta \mathbf{R}_0 &= \delta \mathbf{T}_R^T \mathbf{T}_0 = -\mathbf{R}_0 \delta \mathbf{R}_0^T \mathbf{R}_0 = \mathbf{Spin}(\delta \boldsymbol{\omega}) \mathbf{R}_0 = \mathbf{T}_0^T \mathbf{Spin}(\delta \bar{\boldsymbol{\omega}}) \bar{\mathbf{R}}_0 \mathbf{T}_0, \\ \delta \mathbf{R}_0^T &= \mathbf{T}_0^T \delta \mathbf{T}_R = -\mathbf{R}_0^T \delta \mathbf{R}_0 \mathbf{R}_0^T = -\mathbf{R}_0^T \mathbf{Spin}(\delta \boldsymbol{\omega}) = -\mathbf{T}_0^T \bar{\mathbf{R}}_0^T \mathbf{Spin}(\delta \bar{\boldsymbol{\omega}}) \mathbf{T}_0, \\ \delta \bar{\mathbf{R}}_0 &= \mathbf{T}_0 \delta \mathbf{R}_0 \mathbf{T}_0^T = -\mathbf{T}_0 \mathbf{R}_0 \delta \mathbf{R}_0^T \mathbf{T}_0^T = \mathbf{T}_0 \mathbf{Spin}(\delta \boldsymbol{\omega}) \mathbf{T}_R^T = \mathbf{Spin}(\delta \bar{\boldsymbol{\omega}}) \bar{\mathbf{R}}_0, \\ \delta \bar{\mathbf{R}}_0^T &= \mathbf{T}_0 \delta \mathbf{R}_0^T \mathbf{T}_0^T = -\mathbf{T}_R \delta \mathbf{R}_0 \mathbf{R}_0^T \mathbf{T}_0^T = -\mathbf{T}_R \mathbf{Spin}(\delta \boldsymbol{\omega}) \mathbf{T}_0^T = -\bar{\mathbf{R}}_0^T \mathbf{Spin}(\delta \bar{\boldsymbol{\omega}}). \end{aligned} \quad (12.10)$$

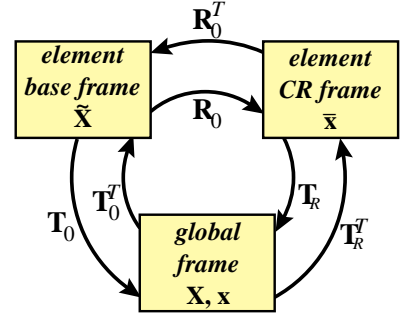


FIGURE 12.8. Rotator frame links.

Table 12.2. Degree of Freedom and Conjugate Force Notation

Notation	Frame	Level	Description
$\hat{\mathbf{v}} = [\hat{\mathbf{v}}_1 \dots \hat{\mathbf{v}}_N]^T$ with $\hat{\mathbf{v}}_a = \begin{bmatrix} \mathbf{u}_a \\ \mathbf{R}_a \end{bmatrix}$	Global	Structure	Total displacements and rotations at structure nodes. Translations: $\mathbf{u}_a$ , rotations: $\mathbf{R}_a$ , for $a = 1, \dots, N$ .
$\delta \mathbf{v} = [\delta \mathbf{v}_1 \dots \delta \mathbf{v}_N]^T$ with $\delta \mathbf{v}_a = \begin{bmatrix} \delta \mathbf{u}_a \\ \delta \boldsymbol{\omega}_a \end{bmatrix}$	Global	Structure	Incremental displacements and spins at structure nodes used in incremental-iterative solution procedure. Translations: $\delta \mathbf{u}_a$ , spins: $\delta \boldsymbol{\omega}_a$ ; conjugate forces: $\mathbf{n}_a$ and $\mathbf{m}_a$ , respectively, for $a = 1, \dots, N$ .
$\delta \bar{\mathbf{v}}^e = [\delta \bar{\mathbf{v}}_1^e \dots \delta \bar{\mathbf{v}}_{N^e}^e]^T$ with $\delta \bar{\mathbf{v}}_a^e = \begin{bmatrix} \delta \bar{\mathbf{u}}_a^e \\ \delta \bar{\boldsymbol{\omega}}_a^e \end{bmatrix}$	Local CR	Element	Localization of above to element $e$ in CR frame. Translations: $\delta \bar{\mathbf{u}}_a^e$ , spins: $\delta \bar{\boldsymbol{\omega}}_a^e$ ; conjugate forces: $\bar{\mathbf{n}}_a^e$ and $\bar{\mathbf{m}}_a^e$ , respectively, for $a = 1, \dots, N^e$ .
$\bar{\mathbf{v}}_d^e = [\bar{\mathbf{v}}_{d1}^e \dots \bar{\mathbf{v}}_{dN^e}^e]^T$ with $\bar{\mathbf{v}}_{da}^e = \begin{bmatrix} \bar{\mathbf{u}}_{da}^e \\ \bar{\boldsymbol{\theta}}_{da}^e \end{bmatrix}$	Local CR	Element	Deformational displacements and rotations at element nodes. Translations: $\bar{\mathbf{u}}_{da}^e$ , rotations: $\bar{\boldsymbol{\theta}}_{da}^e$ ; conjugate forces: $\bar{\mathbf{n}}_a$ and $\bar{\mathbf{m}}_a$ , respectively, for $a = 1, \dots, N^e$ .
$N =$ number of nodes in structure; $N^e =$ number of nodes in element $e$ ; $a, b$ : node indices.			

### §12.3.6. Degrees of Freedom

For simplicity it will be assumed that an  $N^e$ -node CR element has *six degrees of freedom (DOF) per node*: three translations and three rotations. This assumption covers the shell and beam elements evaluated in Part II [R.38]. The geometry of the element is defined by the  $N^e$  coordinates  $\mathbf{x}_a^0$ ,  $a = 1, \dots, N^e$  in the base (initial) configuration, where  $a$  is a node index.

The notation used for DOFs at the structure and element level is collected in Table 12.2. If the structure has  $N$  nodes, the set  $\{\mathbf{u}_a, \mathbf{R}_a\}$  for  $a = 1, \dots, N$  collectively defines the structure node displacement vector  $\mathbf{v}$ . Note, however, that  $\mathbf{v}$  is not a vector in the usual sense because the rotators  $\mathbf{R}_a$  do not transform as vectors when finite rotations are considered. The interpretation as an array of numbers that defines the deformed configuration of elements is more appropriate.

The element total node displacements  $\mathbf{v}^e$  are taken from  $\mathbf{v}$  in the usual manner. Given  $\mathbf{v}^e$ , the key CR operation is to extract the deformational components of the translations and rotations for each node. That sequence of operations is collected in Table 12.3. Note that the computation of the centroid is done by simply averaging the coordinates of the element nodes. For 2-node beams and 3-node triangles this is appropriate. For 4-node quadrilaterals this average does not generally coincide with the centroid, but this has made little difference in actual computations.

### §12.3.7. EICR Matrices

Before studying element deformations, it is convenient to introduce several auxiliary matrices:  $\mathbf{P} = \mathbf{P}_u - \mathbf{P}_\omega$ ,  $\mathbf{S}$ ,  $\mathbf{G}$ ,  $\mathbf{H}$  and  $\mathbf{L}$  that appear in expressions of the EICR front-end. As noted, elements treated here possess  $N^e$  nodes and six degrees of freedom (DOF) per node. The notation and arrangement used for DOFs at different levels is defined in Table 12.2. Subscripts  $a$  and  $b$  denote node indices that run from 1 to  $N^e$ . All EICR matrices are built node-by-node from node-level blocks. Figure 12.9(a) illustrates the concept of perturbed configuration  $\mathcal{C}^D + \delta \mathcal{C}$ , whereas Figure 12.9(b) is used for examples. The CR and deformed configuration are “frozen”; the latter being varied in the sense of variational calculus.

**Table 12.3. Forming the Deformational Displacement Vector.**

Step	Operation for each element $e$ and node $a = 1, \dots, a$
1.	From the initial global nodal coordinates $\mathbf{x}_a^e$ compute centroid position $\mathbf{a}^e = \mathbf{x}_{C_0}^e = (1/N^e) \sum_{a=1}^{N^e} \mathbf{x}_a^e$ . Form rotator $\mathbf{T}_0^e$ as per element type convention. Compute node coordinates in the element base frame: $\bar{\mathbf{x}}_a^e = \mathbf{T}_0^e (\mathbf{x}_a^e - \mathbf{a}^e)$ .
2.	Compute node coordinates in deformed (current) configuration: $\mathbf{x}_a^e = \mathbf{x}_a^e + \mathbf{u}_a^e$ and the centroid position vector $\mathbf{b}^e = \mathbf{x}_C^e = (1/N^e) \sum_{a=1}^{N^e} \mathbf{x}_a^e$ . Establish the deformed local CR system $\mathbf{T}^e$ by a best-fit procedure, and $\mathbf{R}_0^e = \mathbf{T}^e (\mathbf{T}_0^e)^T$ . Form local-CR node coordinates of CR configuration: $\bar{\mathbf{x}}_{Ra}^e = \mathbf{T}^e (\mathbf{x}_a^e - \mathbf{b}^e)$ .
3.	Compute the deformational translations $\bar{\mathbf{u}}_{da} = \bar{\mathbf{x}}_a^e - \bar{\mathbf{x}}_{Ra}^e$ . $\tilde{\mathbf{R}}_d = \mathbf{T}_n \mathbf{R}_a \mathbf{T}_0^T$ . Compute the deformational rotator $\tilde{\mathbf{R}}_{da}^e = \mathbf{T}^e \mathbf{R}_a^e (\mathbf{T}_0^e)^T$ . Extract the deformational angles $\bar{\theta}_{da}^e$ from the axial vector of $\tilde{\mathbf{R}}_{da}^e$ .

The *translational projector matrix*  $\mathbf{P}_u$  or simply *T-projector* is dimensioned  $6N^e \times 6N^e$ . It is built from  $3 \times 3$  numerical submatrices  $\mathbf{U}_{ab} = (\delta_{ab} - 1/N^e) \mathbf{I}$ , in which  $\mathbf{I}$  is the  $3 \times 3$  identity matrix and  $\delta_{ab}$  the Kronecker delta. Collecting blocks for all  $N^e$  nodes and completing with  $3 \times 3$  zero and identity blocks as placeholders for the spins and rotations gives a  $6N^e \times 6N^e$  matrix  $\mathbf{P}_u$ . Its configuration is illustrated below for  $N^e = 2$  (e.g., bar, beam, spar and shaft elements) and  $N^e = 3$  (e.g., triangular shell elements):

$$N_e = 2: \mathbf{P}_u = \begin{bmatrix} \frac{1}{2}\mathbf{I} & \mathbf{0} & -\frac{1}{2}\mathbf{I} & \mathbf{0} \\ \mathbf{0} & \mathbf{I} & \mathbf{0} & \mathbf{0} \\ -\frac{1}{2}\mathbf{I} & \mathbf{0} & \frac{1}{2}\mathbf{I} & \mathbf{0} \\ \mathbf{0} & \mathbf{0} & \mathbf{0} & \mathbf{I} \end{bmatrix}, \quad N_e = 3: \mathbf{P}_u = \begin{bmatrix} \frac{2}{3}\mathbf{I} & \mathbf{0} & -\frac{1}{3}\mathbf{I} & \mathbf{0} & -\frac{1}{3}\mathbf{I} & \mathbf{0} \\ \mathbf{0} & \mathbf{I} & \mathbf{0} & \mathbf{0} & \mathbf{0} & \mathbf{0} \\ -\frac{1}{3}\mathbf{I} & \mathbf{0} & \frac{2}{3}\mathbf{I} & \mathbf{0} & -\frac{1}{3}\mathbf{I} & \mathbf{0} \\ \mathbf{0} & \mathbf{0} & \mathbf{0} & \mathbf{I} & \mathbf{0} & \mathbf{0} \\ -\frac{1}{3}\mathbf{I} & \mathbf{0} & -\frac{1}{3}\mathbf{I} & \mathbf{0} & \frac{2}{3}\mathbf{I} & \mathbf{0} \\ \mathbf{0} & \mathbf{0} & \mathbf{0} & \mathbf{0} & \mathbf{0} & \mathbf{I} \end{bmatrix}. \quad (12.11)$$

For any  $N^e \geq 1$  it is easy to verify that  $\mathbf{P}_u^2 = \mathbf{P}_u$ , with  $5N^e$  unit eigenvalues and  $N^e$  zero eigenvalues. Thus  $\mathbf{P}_u$  is an orthogonal projector. Physically, it extracts the deformational part from the total translational displacements.

Matrix  $\mathbf{S}$  is called the *spin-lever* or *moment-arm* or matrix. It is dimensioned  $3N^e \times 3$  and has the configuration (written in transposed form to save space):

$$\mathbf{S} = [-\mathbf{S}_1^T \quad \mathbf{I} \quad -\mathbf{S}_2^T \quad \mathbf{I} \quad \dots \quad -\mathbf{S}_{N^e}^T \quad \mathbf{I}]^T, \quad (12.12)$$

in which  $\mathbf{I}$  is the  $3 \times 3$  identity matrix and  $\mathbf{S}_a$  are *node spin-lever*  $3 \times 3$  submatrices. Let  $\mathbf{x}_a = [x_{1a} \ x_{2a} \ x_{3a}]^T$  generically denote the 3-vector of coordinates of node  $a$  referred to the element centroid. Then  $\mathbf{S}_a = \mathbf{Spin}(\mathbf{x}_a)$ . The coordinates, however, may be those of three different configurations:  $\mathcal{C}^0$ ,  $\mathcal{C}^R$  and  $\mathcal{C}^D$ , referred to two frame types: global or local. Accordingly superscripts and overbars (or tildes) are used to identify one of six combinations. For example

$$\mathbf{S}_a^0 = \begin{bmatrix} 0 & -x_{3a}^0 - a_3 & x_{2a}^0 - a_2 \\ x_{3a}^0 - a_3 & 0 & -x_{1a}^0 - a_1 \\ -x_{2a}^0 - a_2 & x_{1a}^0 - a_1 & 0 \end{bmatrix}, \quad \bar{\mathbf{S}}_a^R = \begin{bmatrix} 0 & -\bar{x}_{3a}^R & \bar{x}_{2a}^R \\ \bar{x}_{3a}^R & 0 & -\bar{x}_{1a}^R \\ -\bar{x}_{2a}^R & \bar{x}_{1a}^R & 0 \end{bmatrix}, \quad \bar{\mathbf{S}}_a^D = \begin{bmatrix} 0 & -\bar{x}_{3a}^D & \bar{x}_{2a}^D \\ \bar{x}_{3a}^D & 0 & -\bar{x}_{1a}^D \\ -\bar{x}_{2a}^D & \bar{x}_{1a}^D & 0 \end{bmatrix}, \quad (12.13)$$

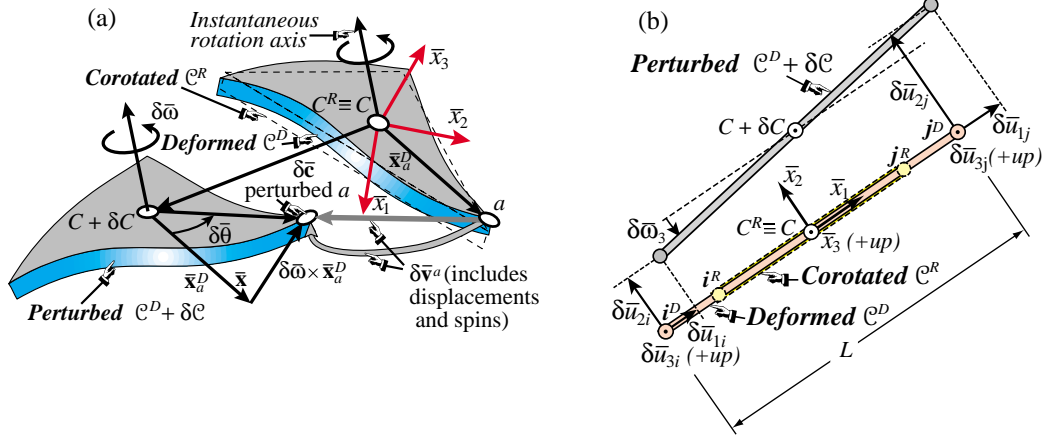


FIGURE 12.9. Concept of perturbed configuration to illustrate derivation of EICR matrices: (a) facet triangular shell element moving in 3D space; (b) 2-node bar element also in 3D but depicted in the  $\{\bar{x}_1, \bar{x}_2\}$  plane of its CR frame. Deformations grossly exaggerated for visualization convenience; strains and local rotations are in fact infinitesimal.

are node spin-lever matrices for base-in-global-frame, CR-in-local-frame and deformed-in-local-frame, respectively. The element matrix (12.12) inherits the notation; in this case  $\mathbf{S}^0$ ,  $\bar{\mathbf{S}}^R$  and  $\bar{\mathbf{S}}^D$ , respectively. For instance,  $\mathbf{S}$  matrices for the 2-node space  $i - j$  bar element pictured in Figure 12.9(b) are  $12 \times 3$ . If the length of the bar in  $\mathcal{C}^D$  is  $L$ , the deformed bar spin-lever matrix referred to the local CR frame is

$$\bar{\mathbf{S}}^D = \frac{1}{2}L \begin{bmatrix} 0 & 0 & 0 & 0 & 0 & 0 & 0 & 0 & 0 & 0 & 0 & 0 \\ 0 & 0 & 1 & 0 & 0 & 0 & 0 & 0 & -1 & 0 & 0 & 0 \\ 0 & -1 & 0 & 0 & 0 & 0 & 0 & 0 & 1 & 0 & 0 & 0 \end{bmatrix}^T. \quad (12.14)$$

The first row is identically zero because the torque about the bar axis  $\bar{x}_1$  vanishes in straight bar models. Matrix  $\mathbf{G}$ , introduced by Haugen [R.37], is dimensioned  $3 \times 6N^e$ , and will be called the *spin-fitter* matrix. It links variations in the element spin (instantaneous rotations) at the *centroid of the deformed configuration* in response to variations in the nodal DOFs. See Figure 12.9(a).  $\mathbf{G}$  comes in two flavors, global and local:

$$\delta\boldsymbol{\omega} \stackrel{\text{def}}{=} \mathbf{G} \delta\mathbf{v}^e = \sum_a \mathbf{G}_a \delta\mathbf{v}_a^e, \quad \delta\bar{\boldsymbol{\omega}} \stackrel{\text{def}}{=} \bar{\mathbf{G}} \delta\bar{\mathbf{v}}^e = \sum_a \bar{\mathbf{G}}_a \delta\bar{\mathbf{v}}_a^e, \quad \text{with} \quad \sum_a \equiv \sum_{a=1}^{N^e}. \quad (12.15)$$

Here the spin axial vector variation  $\delta\boldsymbol{\omega}^e$  denotes the instantaneous rotation at the centroid, measured in the global frame, when the deformed configuration is varied by the  $6N^e$  components of  $\delta\mathbf{v}^e$ . When referred to the local CR frame, these become  $\delta\bar{\boldsymbol{\omega}}^e$  and  $\delta\bar{\mathbf{v}}^e$ , respectively. For construction, both  $\mathbf{G}$  and  $\bar{\mathbf{G}}$  may be split into node-by-node contributions using the  $3 \times 6$  submatrices  $\mathbf{G}_a$  and  $\bar{\mathbf{G}}_a$  shown above. As an example,  $\mathbf{G}$  matrices for the space bar element shown in Figure 12.9(b) is  $3 \times 12$ . The spin-lever matrix in  $\mathcal{C}^D$  referred to the local CR frame is

$$\bar{\mathbf{G}}^D = \frac{1}{L} \begin{bmatrix} 0 & 0 & 0 & 0 & 0 & 0 & 0 & 0 & 0 & 0 & 0 & 0 \\ 0 & 0 & 1 & 0 & 0 & 0 & 0 & 0 & -1 & 0 & 0 & 0 \\ 0 & -1 & 0 & 0 & 0 & 0 & 0 & 0 & 1 & 0 & 0 & 0 \end{bmatrix}. \quad (12.16)$$

The first row is conventionally set to zero as the spin about the bar axis  $\bar{x}_1$  is not defined by the nodal freedoms. This “torsion spin” is defined, however, in 3D beam models by the end torsional rotations.

Unlike  $\mathbf{S}$ , the entries of  $\mathbf{G}$  depend not only on the element geometry, but on a developer's decision: how the CR configuration  $\mathcal{C}^R$  is fitted to  $\mathcal{C}^D$ . For the triangular shell element this matrix is given in Appendix B. For quadrilateral shells and space beam elements it is given in Part II [R.38].

Matrices  $\bar{\mathbf{S}}^D$  and  $\bar{\mathbf{G}}^D$  satisfy the biorthogonality property

$$\mathbf{G}\mathbf{S} = \mathbf{D}. \quad (12.17)$$

where  $\mathbf{D}$  is a  $3 \times 3$  diagonal matrix of zeros and ones. A diagonal entry of  $\mathbf{D}$  is zero if a spin component is undefined by the element freedoms. For instance in the case of the space bar, the product  $\bar{\mathbf{G}}^D \bar{\mathbf{S}}^D$  of (12.14) and (12.16) is **diag**(0, 1, 1). Aside from these special elements (e.g., bar, spars, shaft elements),  $\mathbf{D} = \mathbf{I}$ . This property results from the fact that the three columns of  $\mathbf{S}$  are simply the displacement vectors associated with the rigid body rotations  $\delta\bar{\omega}_i = 1$ . When premultiplied by  $\mathbf{G}$  one merely recovers the amplitudes of those three modes.

The *rotational projector* or simply *R-projector* is generically defined as  $\mathbf{P}_\omega = \mathbf{S}\mathbf{G}$ . Unlike the T-projector  $\mathbf{P}_u$  such as those in (12.11), the R-projector depends on configuration and frame of reference. Those are identified in the usual manner; e.g.,  $\bar{\mathbf{P}}_\omega^R = \bar{\mathbf{S}}_\omega^R \bar{\mathbf{G}}_\omega^R$ . This  $6N^e \times 6N^e$  matrix is an orthogonal projector of rank equal to that of  $\mathbf{D} = \mathbf{G}\mathbf{S}$ . If  $\mathbf{G}\mathbf{S} = \mathbf{I}$ ,  $\mathbf{P}_r$  has rank 3. The complete *projector matrix* of the element is defined as

$$\mathbf{P} = \mathbf{P}_u - \mathbf{P}_\omega. \quad (12.18)$$

This is shown to be a projector, that is  $\mathbf{P}^2 = \mathbf{P}$ , in Section 4.2.

Two additional  $6N^e \times 6N^e$  matrices, denoted by  $\mathbf{H}$  and  $\mathbf{L}$ , appear in the EICR.  $\mathbf{H}$  is a block diagonal matrix built of  $2N^e$   $3 \times 3$  blocks:

$$\mathbf{H} = \mathbf{diag}[\mathbf{I} \mathbf{H}_1 \mathbf{I} \mathbf{H}_2 \dots \mathbf{I} \mathbf{H}_{N^e}], \quad \mathbf{H}_a = \mathbf{H}(\theta_a), \quad \mathbf{H}(\theta) = \partial\theta/\partial\omega. \quad (12.19)$$

Here  $\mathbf{H}_a$  denotes the Jacobian derivative of the rotational axial vector with respect to the spin axial vector evaluated at node  $a$ . An explicit expression of  $\mathbf{H}(\theta)$  is given in (R.48) of Appendix A. The local version in the CR frame is

$$\bar{\mathbf{H}} = \mathbf{diag}[\mathbf{I} \bar{\mathbf{H}}_{d1} \mathbf{I} \bar{\mathbf{H}}_{d2} \dots \mathbf{I} \bar{\mathbf{H}}_{dN^e}], \quad \bar{\mathbf{H}}_{da} = \bar{\mathbf{H}}(\bar{\theta}_{da}), \quad \bar{\mathbf{H}}(\bar{\theta}_d) = \partial\bar{\theta}_d/\partial\bar{\omega}_d. \quad (12.20)$$

$\mathbf{L}$  is a block diagonal matrix built of  $2N^e$   $3 \times 3$  blocks:

$$\mathbf{L} = \mathbf{diag}[\mathbf{0} \mathbf{L}_1 \mathbf{0} \mathbf{L}_2 \dots \mathbf{0} \mathbf{L}_{N^e}], \quad \mathbf{L}_a = \mathbf{L}(\theta_a, \mathbf{m}_a). \quad (12.21)$$

where  $\mathbf{m}_a$  is the 3-vector of moments (conjugate to  $\delta\omega_a$ ) at node  $a$ . The expression of  $\mathbf{L}(\theta, \mathbf{m})$  is provided in (R.49) of Appendix A. The local form  $\bar{\mathbf{L}}$  has the same block organization with  $\mathbf{L}_a$  replaced by  $\bar{\mathbf{L}}_a = \mathbf{L}(\bar{\theta}_{da}, \bar{\mathbf{m}}_a)$ .

### §12.3.8. Deformational Translations

Consider a generic point  $P^0$  of the base element of Figure 12.5, with global position vector  $\mathbf{x}_p^0$ .  $P^0$  rigidly moves to  $P^R$  in  $\mathcal{C}^R$  with position vector  $\mathbf{x}_p^R = \mathbf{x}_p^0 + \mathbf{u}_p^R = \mathbf{x}_p^0 + \mathbf{c} + \mathbf{x}_{pC}^R$ . Next the element deforms to occupy  $\mathcal{C}^D$ .  $P^R$  displaces to  $P$ , with global position vector  $\mathbf{x}_p = \mathbf{x}_p^0 + \mathbf{u}_p = \mathbf{x}_p^0 + \mathbf{c} + \mathbf{x}_{pC}^R + \mathbf{u}_{dP}$ .

The global vector from  $C^0$  to  $P^0$  is  $\mathbf{x}_p^0 - \mathbf{a}$ , which in the base frame becomes  $\bar{\mathbf{x}}_p^0 = \mathbf{T}_0(\mathbf{x}_p^0 - \mathbf{a})$ . The global vector from  $C^R \equiv C$  to  $P^R$  is  $\mathbf{x}_p^R - \mathbf{b}$ , which in the element CR frame becomes  $\bar{\mathbf{x}}_p^R = \mathbf{T}_R(\mathbf{x}_{pC}^R - \mathbf{b})$ .

But  $\tilde{\mathbf{x}}_P^0 = \bar{\mathbf{x}}_P^R$  since the  $\mathcal{C}^0 \rightarrow \mathcal{C}^R$  motion is rigid. The global vector from  $P_R$  to  $P$  is  $\mathbf{u}_{dP} = \mathbf{x}_P - \mathbf{x}_P^R$ , which represents a deformational displacement. In the CR frame this becomes  $\bar{\mathbf{u}}_{dP} = \mathbf{T}_R(\mathbf{x}_P - \mathbf{x}_P^R)$ .

The total displacement vector is the sum of rigid and deformational parts:  $\mathbf{u}_P = \mathbf{u}_{rP} + \mathbf{u}_{dP}$ . The rigid displacement is given by expressions collected in (12.5), of which  $\mathbf{u}_{rP} = (\mathbf{R}_0 - \mathbf{I})(\mathbf{x}_P^0 - \mathbf{a}) + \mathbf{c}$  is the most useful. The deformational part is extracted as  $\mathbf{u}_{dP} = \mathbf{u}_P - \mathbf{u}_{rP} = \mathbf{u}_P - \mathbf{c} + (\mathbf{I} - \mathbf{R}_0)(\mathbf{x}_P^0 - \mathbf{a})$ . Dropping  $P$  to reduce clutter this becomes

$$\mathbf{u}_d = \mathbf{u} - \mathbf{c} + (\mathbf{I} - \mathbf{R}_0)(\mathbf{x}^0 - \mathbf{a}). \quad (12.22)$$

The element centroid position is calculated by averaging its node coordinates. Consequently

$$\mathbf{c} = (1/N^e) \sum_b \mathbf{u}_b, \quad \mathbf{u}_a - \mathbf{c} = \sum_b \mathbf{U}_{ab} \mathbf{u}_b, \quad \text{with} \quad \sum_b \equiv \sum_{b=1}^{N^e} \quad (12.23)$$

in which  $\mathbf{U}_{ab} = (\delta_{ab} - 1/N^e)\mathbf{I}$  is a building block of the T-projector introduced in the foregoing subsection. Evaluate (12.22) at node  $a$ , insert (12.23), take variations using (12.10) to handle  $\delta\mathbf{R}_0$ , use (12.2) to map  $\mathbf{R}_0(\mathbf{x}^0 - \mathbf{a}) = \mathbf{x}^R - \mathbf{b}$ , and employ the cross-product skew-symmetric property (R.3) to extract  $\delta\boldsymbol{\omega}$ :

$$\begin{aligned} \delta\mathbf{u}_{da} &= \delta(\mathbf{u}_a - \mathbf{c}) - \delta\mathbf{R}_0(\mathbf{x}_a^0 - \mathbf{a}) = \sum_b \mathbf{U}_{ab} \delta\mathbf{u}_b - \mathbf{Spin}(\delta\boldsymbol{\omega}) \mathbf{R}_0(\mathbf{x}_a^0 - \mathbf{a}) \\ &= \sum_b \mathbf{U}_{ab} \delta\mathbf{u}_b - \mathbf{Spin}(\delta\boldsymbol{\omega})(\mathbf{x}_a^R - \mathbf{b}) = \sum_b \mathbf{U}_{ab} \delta\mathbf{u}_b + \mathbf{Spin}(\mathbf{x}_a^R - \mathbf{b}) \delta\boldsymbol{\omega} \\ &= \sum_b \mathbf{U}_{ab} \delta\mathbf{u}_b + \sum_b \mathbf{S}_a^R \mathbf{G}_b \delta\mathbf{v}_b. \end{aligned} \quad (12.24)$$

Here matrices  $\mathbf{S}$  and  $\mathbf{G}$  have been introduced in (12.12)–(12.15). The deformational displacement in the element CR frame is  $\bar{\mathbf{u}}_d = \mathbf{T}_R \mathbf{u}_d$ . From the last of (12.5) we get  $\bar{\mathbf{u}}_d = \bar{\mathbf{u}} - \bar{\mathbf{c}} - (\mathbf{I} - \bar{\mathbf{R}}_0^T) \bar{\mathbf{x}}^R$ , where  $\bar{\mathbf{R}}_0 = \mathbf{T}_R \mathbf{R}_0 \mathbf{T}_R^T$ . Proceeding as above one gets

$$\delta\bar{\mathbf{u}}_{da} = \sum_b \mathbf{U}_{ab} \delta\bar{\mathbf{u}}_b + \sum_b \bar{\mathbf{S}}_a^D \bar{\mathbf{G}}_b \delta\bar{\mathbf{v}}_b. \quad (12.25)$$

The node lever matrix  $\mathbf{S}_a^R$  of (12.24) changes in (12.25) to  $\bar{\mathbf{S}}_a^D$ , which uses the node coordinates of the *deformed* element configuration.

### §12.3.9. Deformational Rotations

Denote by  $\mathbf{R}_P$  the rotator associated with the motion of the material particle originally at  $P^0$ ; see Figure 12.6. Proceeding as in the translational analysis this is decomposed into the rigid rotation  $\mathbf{R}_0$  and a deformational rotation:  $\mathbf{R}_P = \mathbf{R}_{dP} \mathbf{R}_0$ . The sequence matters because  $\mathbf{R}_{dP} \mathbf{R}_0 \neq \mathbf{R}_0 \mathbf{R}_{dP}$ . The order  $\mathbf{R}_{dP} \mathbf{R}_0$ : rigid rotation follows by deformation, is consistent with those used by Bergan, Rankin and coworkers; e.g. [R.54,R.56]. (From the standpoint of continuum mechanics based on the polar decomposition theorem [R.81, Sec. 37] the left stretch measure is used.) Thus  $\mathbf{R}_{dP} = \mathbf{R}_P \mathbf{R}_0^T$ , which can be mapped to the local CR system as  $\bar{\mathbf{R}}_d = \mathbf{T}_R \mathbf{R}_d \mathbf{T}_R^T$ . Dropping the label  $P$  for brevity we get

$$\mathbf{R}_d = \mathbf{R} \mathbf{R}_0^T = \mathbf{R} \mathbf{T}_0^T \mathbf{T}_R, \quad \bar{\mathbf{R}}_d = \mathbf{T}_R \mathbf{R}_d \mathbf{T}_R^T = \mathbf{T}_R \mathbf{R} \mathbf{T}_0^T. \quad (12.26)$$

The deformational rotation (12.26) is taken to be small but finite. Thus a procedure to extract a rotation axial vector  $\theta_d$  from a given rotator is needed. Formally this is  $\bar{\boldsymbol{\theta}}_d = \mathbf{axial}[\mathbf{Log}_e(\bar{\mathbf{R}}_d)]$ , but this can be prone to numerical instabilities. A robust procedure is presented in Section A.11. The axial vector is evaluated at the nodes and identified with the rotational DOF.

Evaluating (12.26) at a node  $a$ , taking variations and going through an analysis similar to that carried out in the foregoing section yields

$$\begin{aligned}\delta\boldsymbol{\theta}_{da} &= \frac{\partial\boldsymbol{\theta}_{da}}{\partial\boldsymbol{\omega}_{da}} \sum_b \frac{\partial\boldsymbol{\omega}_{da}}{\partial\boldsymbol{\omega}_b} \delta\boldsymbol{\omega}_b = \mathbf{H}_a \sum_b (\delta_{ab} [\mathbf{0} \quad \mathbf{I}] - \mathbf{G}_b) \delta\mathbf{v}_b. \\ \delta\bar{\boldsymbol{\theta}}_{da} &= \frac{\partial\bar{\boldsymbol{\theta}}_{da}}{\partial\bar{\boldsymbol{\omega}}_{da}} \sum_b \frac{\partial\bar{\boldsymbol{\omega}}_{da}}{\partial\bar{\boldsymbol{\omega}}_b} \delta\bar{\boldsymbol{\omega}}_b = \bar{\mathbf{H}}_a \sum_b (\delta_{ab} [\mathbf{0} \quad \mathbf{I}] - \bar{\mathbf{G}}_b) \delta\bar{\mathbf{v}}_b.\end{aligned}\tag{12.27}$$

where  $\mathbf{G}_b$  is defined in (12.15) and  $\mathbf{H}_a$  in (12.19).

---

Overview continues in next Chapter.